STAR Protocols

CellPress
OPEN ACCESS

Protocol

Measurement of cerebral oxygen pressure in living mice by two-photon phosphorescence lifetime microscopy

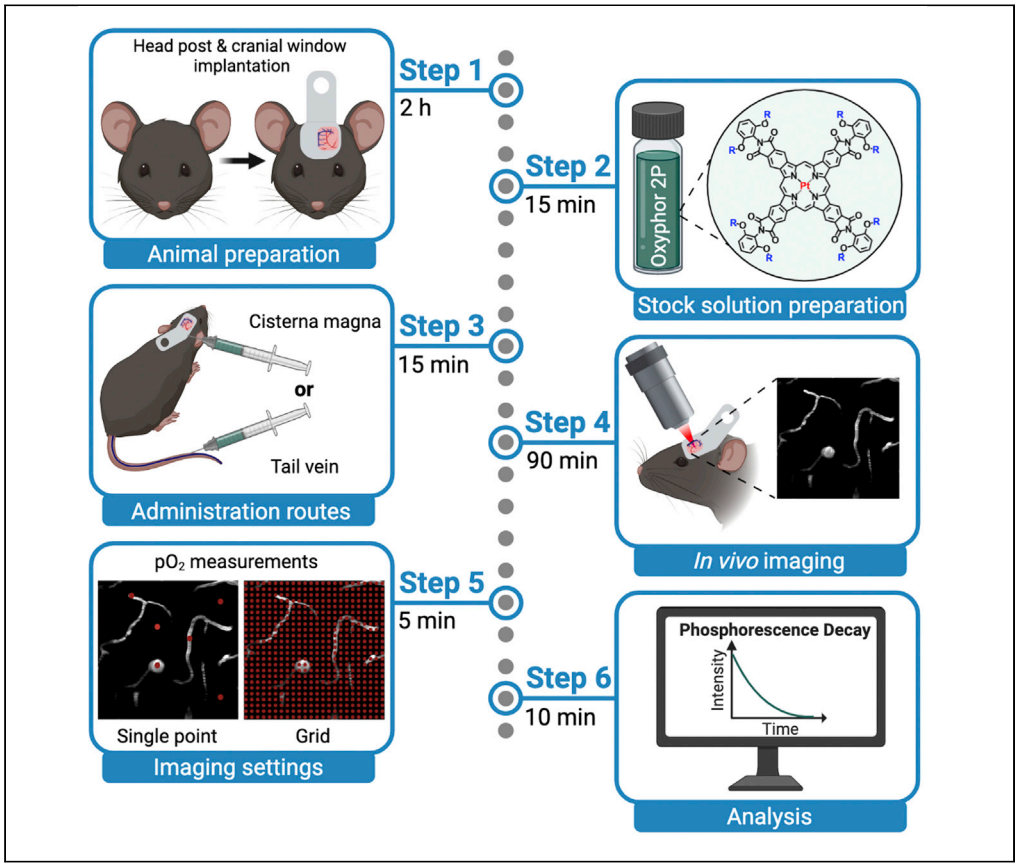

The ability to quantify partial pressure of oxygen (pO_2) is of primary importance for studies of metabolic processes in health and disease. Here, we present a protocol for imaging of oxygen distributions in tissue and vasculature of the cerebral cortex of anesthetized and awake mice. We describe *in vivo* two-photon phosphorescence lifetime microscopy (2PLM) of oxygen using the probe Oxyphor 2P. This minimally invasive protocol outperforms existing approaches in terms of accuracy, resolution, and imaging depth.

Eva Erlebach, Luca Ravotto, Matthias T. Wyss, Jacqueline Condrau, Thomas Troxler, Sergei A. Vinogradov, Bruno Weber

vinograd.upenn@gmail.com (S.A.V.)
bweber@pharma.uzh.ch (B.W.)

Highlights

Two-photon phosphorescence imaging of Oxyphor 2P allows for oxygen measurement *in vivo*

Oxygen imaging can be performed in anesthetized or awake, behaving mice

Intravenous injection enables oxygen imaging in the vasculature

Cisterna magna injection enables extra- and intravascular oxygen imaging in the brain

Erlebach et al., STAR Protocols *3*, 101370
June 17, 2022
https://doi.org/10.1016/j.xpro.2022.101370

STAR Protocols

CellPress
OPEN ACCESS

Protocol

Measurement of cerebral oxygen pressure in living mice by two-photon phosphorescence lifetime microscopy

Eva Erlebach,[1,4] Luca Ravotto,[1,4] Matthias T. Wyss,[1] Jacqueline Condrau,[1] Thomas Troxler,[2,3] Sergei A. Vinogradov,[2,3,5,*] and Bruno Weber[1,6,*]

[1]Institute of Pharmacology and Toxicology, University of Zurich, 8057 Zürich, Switzerland

[2]Department of Biochemistry and Biophysics, Perelman School of Medicine, University of Pennsylvania, Philadelphia, PA 19104, USA

[3]Department of Chemistry, School of Arts and Sciences, University of Pennsylvania, Philadelphia, PA 19104, USA

[4]These authors contributed equally

[5]Technical contact

[6]Lead contact

*Correspondence: vinograd.upenn@gmail.com (S.A.V.), bweber@pharma.uzh.ch (B.W.)
https://doi.org/10.1016/j.xpro.2022.101370

SUMMARY

The ability to quantify partial pressure of oxygen (pO_2) is of primary importance for studies of metabolic processes in health and disease. Here, we present a protocol for imaging of oxygen distributions in tissue and vasculature of the cerebral cortex of anesthetized and awake mice. We describe *in vivo* two-photon phosphorescence lifetime microscopy (2PLM) of oxygen using the probe Oxyphor 2P. This minimally invasive protocol outperforms existing approaches in terms of accuracy, resolution, and imaging depth.

For complete details on the use and execution of this protocol, please refer to Esipova et al. (2019).

BEFORE YOU BEGIN

This protocol describes the quantification of the partial pressure of oxygen (pO_2) in the brain tissue *in vivo* by means of two-photon phosphorescence lifetime microscopy (2PLM) (Finikova et al., 2008; Sakadžić et al., 2010; Parpaleix et al., 2011). Oxygen is an efficient quencher of phosphorescence, and the phosphorescence decay time, or simply phosphorescence lifetime, of an exogenous probe can serve as a proxy for oxygen concentration (Vanderkooi et al., 1987).

The phosphorescent probe Oxyphor 2P (Esipova et al., 2019) was recently reported as a major improvement over the previous generation of two-photon-excitable oxygen probes (Briñas et al., 2005; Finikova et al., 2008; Roussakis et al., 2014). The chemical structure of Oxyphor 2P makes its signal highly specific for oxygen in biological environments, allowing for measurements of absolute oxygen concentrations. The dependence of the phosphorescence lifetime on pO_2 and temperature is given by an empirical expression with coefficients determined during calibration experiments (Esipova et al., 2019).

In a 2PLM experiment, molecules of Oxyphor 2P near the focal point of the microscope objective are excited by a short train of near-infrared femtosecond laser pulses, and the resulting decay of phosphorescence intensity is recorded as a function of time. A series of excitation/collection cycles are executed to increase the signal-to-noise ratio (SNR), after which the phosphorescence lifetime is calculated and converted to the local pO_2. The combination of near-focal two-photon excitation with insensitivity of microscopic phosphorescence lifetime-based measurements to optical properties of the medium (tissue absorption and scattering) allows for accurate quantification of pO_2 in living tissue with sub-micrometer spatial accuracy (Esipova et al., 2019).

Below, we describe a protocol for using 2PLM and Oxyphor 2P to map oxygen levels in the vasculature and extravascular space in the cerebral cortex of mice.

All experiments were approved by the local veterinary authorities according to the guidelines of the Swiss Animal Protection Law, Veterinary Office, Canton Zurich (Animal Welfare Act, 16 December 2005 and Animal Welfare Ordinance, 23 April 2008).

Animal preparation

Timing: 3–4 days

Several methods exist for head fixation and cranial window implantation in mice (Holtmaat et al., 2009; Kılıç et al., 2021). All such methods are appropriate if they permit longitudinal two-photon imaging. Below we describe a method developed in our laboratory (Esipova et al., 2019; Zuend et al., 2020).

⚠ CRITICAL: All animal experiments must be performed in accordance with the guidelines and regulations at the respective institutions.

Head post implantation

Timing: 1 h

1. Anaesthetize the animal with isoflurane (4% induction, 1.5%–3% for maintenance) mixed with oxygen/air (30%/70%).
2. Inject buprenorphine (0.1 mg/kg, subcutaneous [s.c.]) for analgesia.
3. Protect the eyes from dehydration and irritation by applying a Vitamin A ointment (Vitamin A Blache Augensalbe, Bausch & Lomb Swiss AG). The application is repeated as often as necessary.
4. Shave the head and disinfect (Kodan®, Schülke & Mayr AG) the skin three times.
5. Place the animal on a heating pad to prevent hypothermia and affix the animal's head in a stereotaxic frame. Breathing rate should also be monitored regularly during the entire duration of anesthesia.

⚠ CRITICAL: Use a heating pad with feedback control to ensure that the animal's body temperature is kept constant (~37°C).

6. Inject local anesthesia s.c. using lidocaine/bupivacaine (50 μL of stock solution, consisting of lidocaine (1 mL, 20 mg/mL) and bupivacaine (1 mL, 5 mg/mL), mixed in saline (1 mL)).
7. Expose the skull by performing a midline skin incision (length: ~12 mm) from between the eyes to the level of the ears.
8. Softly remove the periosteum with the help of a raspatorium and clean the exposed skull and remove the periosteum.
9. Spread a bonding agent (One Coat 7 universal, Coltene) over the exposed skull calvaria while sparing the area designated for later craniotomy.
10. Form a head cap by layer-by-layer application of a light-curing dental composite (Tetric EvoFlow®, Ivoclar Vivadent) over the region treated with the bonding agent (Figure 1A, left).
11. After applying each layer, illuminate the composite with blue curing light for 15 s (e.g., LED.F, Woodpecker®).

Note: In the end, the head cap should cover the previously exposed skull except for the cranial area at the site of subsequent craniotomy on one hemisphere.

12. Using the dental composite, attach a custom-made aluminum head post to the back of the head cap (Figure 1A, right) behind the area reserved for craniotomy leaving enough space for the

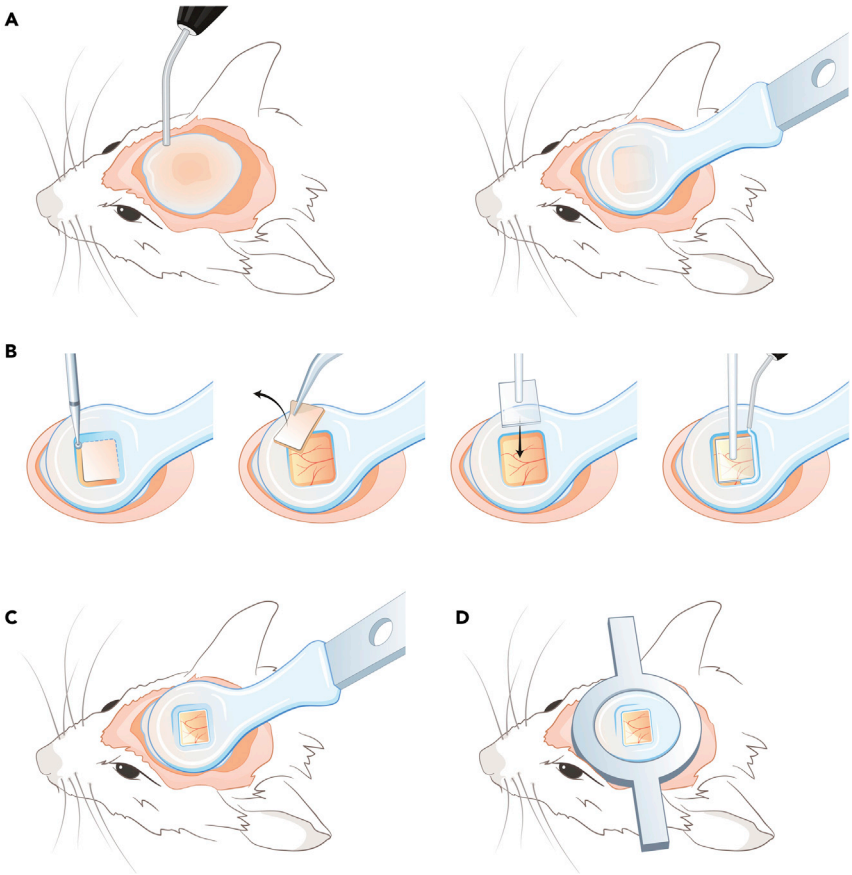

Figure 1. Implantation of head post and chronic window

(A) Application of dental composite on the exposed and clean skull to form a head cap (left panel) and to attach a custom-made aluminum head post (right panel; size of the head post: 6 × 14 mm).

(B) Using a dental drill, the outline of the cranial window is thinned until the bone piece can be removed with a forceps. In a next step a clean cover glass window (3 × 3 mm) is placed on the exposed area and fixed with dental composite.

(C and D) represent the final stage with glass window implanted in place either with head post (D) or head plate (D).

objective. This helps for keeping the mouse in a more comfortable posture during imaging and ensures that the entire cranial window area can be imaged.

13. To prevent infections and to facilitate wound healing, pull the retracted skin back over the border of the head cap and fix it with a tissue adhesive (Histoacryl®, B. Braun); finally apply antibiotic ointment (Fucidin®, LEO Pharma GmbH) at the site of attachment between the skin and the composite.
14. Inject prewarmed Ringerfundin® (0.01 mL/g body weight, s.c.) to prevent dehydration.
15. Stop anesthesia and monitor the animal until it fully recovers in a heated recovery cage.
16. Continue analgesia using buprenorphine for at least 2–3 days after surgery (daytime: 0.1 mg/kg, s.c. every 6 h; during the night: 5 mL buprenorphine (0.3 mg/mL) diluted in 160 mL drinking water).

⚠ CRITICAL: The mouse should be allowed to recover for 2–3 days after the head post attachment surgery prior to the cranial window implantation. Usually, mice recover faster if surgical procedures are split into two sessions.

Note: Head post implantation and craniotomy plus chronic window implantation could also be performed on the same day.

Cranial window implantation

Timing: 1 h

17. Using a microbrush, thoroughly clean a sapphire glass window (3 × 3 mm; HEBO Spezialglas, cut by Powatec GmbH) that will be implanted over the craniotomy area, using ethanol 100% and distilled water in sequence.
18. Cover the edges of the glass window with a thin layer of the dental composite (Tetric EvoFlow®, Ivoclar Vivadent) and cure it with the curing light (e.g., LED.F, Woodpecker®).

Note: Protect the prepared window from dust.

19. Anaesthetize the animal with a mixture of midazolam, medetomidine and fentanyl (5/0.5/0.05 mg/kg body weight, intraperitoneal (i.p.) injection) and place it on a heating pad. Use the aluminum head post to fix the animal's head on a custom-made holder for the subsequent surgery.
20. Protect the animal's eyes from dehydration and irritation by applying Vitamin A ointment (Vitamin A Blache Augensalbe, Bausch & Lomb Swiss AG). The application is repeated as often as necessary.

⚠ CRITICAL: Use a heating pad with feedback control to ensure that the animal's body temperature is kept constant (~37°C).

21. Flush the head cap and the uncovered skull area reserved for craniotomy with Ringer solution.
22. Using a dental drill (diameter 0.2 mm, H-4-002 HP, Rotatec GmbH), thin the bone within the outline of the cranial window (Figure 1B, first step) on the left parietal calvaria (recessed part of the head cap). Stop drilling when a thin layer of bone is left (~0.1–0.2 mm) and carefully lift that remaining bone layer with a thin forceps without touching the brain (Figure 1B, second step).

Note: While performing the craniotomy, stop at least every 2 min and cool the skull with Ringer solution or a flow of air.

⚠ CRITICAL: When performing the craniotomy, avoid drilling in the same area for more than 2 s and use an air flow to prevent overheating, otherwise bleeding may occur underneath the skull.

⚠ CRITICAL: Make sure to keep the dura mater intact during bone removal. After removal of the bone, keep the dura mater moist at all times by applying Ringer solution.

⚠ CRITICAL: An injury of the brain cortex or/and a subpial bleeding during the craniotomy would be considered as an experiment endpoint.

23. Place the prepared sapphire glass window gently on top of the exposed brain (Figure 1B, third step).

Note: Apply a drop of Ringer solution to the exposed brain before covering it with the glass window. The layer of liquid between the glass and the brain surface will make it easier to adjust the position of the window.

24. Gently press on the glass window to ensure that the entire exposed area of the brain is in contact with the glass, while the window is properly aligned with respect to the surrounding skull.
25. Using Sugi® swabs (Kettenbach GmbH, Eschenburg Germany) to carefully dry the area surrounding the window.
26. Affix the glass window to the head cap with the dental composite (Figure 1B, fourth step).
27. Inject saline (0.01 mL/g body weight, s.c.) to prevent dehydration, flumazenil/atipamezole (0.1/5 mg/kg, s.c.) to antagonize anesthesia and buprenorphine (0.1 mg/kg, s.c.) for analgesia.

28. Monitor the animal until it fully recovers from the anesthesia.
29. Continue analgesia using buprenorphine for at least 2–3 days after surgery (daytime: 0.1 mg/kg, s.c. every 6 h; during the night: 5 mL buprenorphine (0.3 mg/mL) diluted in 160 mL drinking water).

⚠ CRITICAL: The mouse should be allowed to recover for at least 1 week after the cranial window implantation prior to imaging.

⚠ CRITICAL: If the window appears unclear (for example, due to an inflammatory process), the experiment should be terminated.

Preparation of stock solution of Oxyphor 2P

Timing: 15 min

Oxyphor 2P is distributed either as a stock solution (typically 200–500 μM) or as a solid, from which the required stock solutions should be prepared.

Note: If you are performing intravenous (i.v.) injection, proceed to steps 30 and 31. If you are performing injection into cisterna magna, proceed to steps 32 and 33.

Stock solution for intravenous (i.v.) injection

30. Dissolve solid Oxyphor 2P in saline to the final concentration (cSS) of 250 μM.
31. Divide the resulting stock solution into appropriate aliquots (50–100 μL) and store them in the dark frozen at −20°C.

Stock solution for injection into cisterna magna

32. Dissolve solid Oxyphor 2P in Ringer solution to the final concentration of 1.1–1.2 mM.
33. Divide the stock solution into 11–12 μL aliquots and store them in the dark frozen at −20°C.

Note: The molecular weight of Oxyphor 2P is ~75 kDa (Esipova et al., 2019).

⚠ CRITICAL: Solid Oxyphor 2P can absorb water during storage. It is advised to verify the actual concentrations of prepared solutions spectrophotometrically. According to the Beer-Lambert law:

$$c = \frac{A_{630}}{\epsilon_{630} \cdot l}$$

where c is the molar concentration (mole/L), A_{630} is the absorbance of the probe solution at 630 nm, ϵ_{630} is the molar absorption coefficient at 630 nm (ϵ_{630} = 275,000 $M^{-1}cm^{-1}$ (Esipova et al., 2019) and l is the optical path length in cm.

KEY RESOURCES TABLE

REAGENT or RESOURCE	SOURCE	IDENTIFIER
Chemicals, peptides, and recombinant proteins		
Atipamezole	Virbac (Switzerland) AG	Revertor ad us vet 5 mg/mL; ATCvet: QV03AB90
Bupivacaine 0.5%	Sintetica SA	GTIN: 7680557270311
Buprenorphine	Indivior Schweiz AG	Temgesic®, 0.3 mg/mL; GTIN: 7680419310018

(*Continued on next page*)

Continued

REAGENT or RESOURCE	SOURCE	IDENTIFIER
Disinfectant (Kodan®)	Schülke & Mayr AG	Cat#104022; GTIN: 7680441570718
Fentanyl	Sintetica®	0.1 mg/2 mL; GTIN: 7680539870010
FITC Dextran (70 kDa)	Sigma-Aldrich	FD70; CAS: 60842-46-8
Flumazenil	Sintetica SA	Flumazenil 0.5 mg/mL; GTIN: 7680584760052
Fucidin Crème 2%	LEO Pharma GmbH	GTIN: 7680468980286
Isoflurane	Piramal Critical Care	Attane™, 250 mL; ATCvet: QN01AB06
Lidocaine	Streuli®	2%, 40 mg/ 2 mL; GTIN: 7680300165130
Medetomidine	Orion Pharma	Domitor®, 10 mL; ATCvet: QN05CM91
Midazolam	CPS Cito Pharma Services GmbH	Dormicum 15 mg/ 3 mL
NaCl (0.9%)	B.Braun Medical AG	GTIN: 7680295542268
Oxyphor 2P	Esipova et al. (2019)	N/A
Ringer	B.Braun Medical AG	GTIN: 7680382052694
Ringerfundin®	B.Braun Medical AG	GTIN: 7680574340011
Vitamin A Blache Augensalbe	Bausch & Lomb Swiss AG	GTIN: 7680223980247
Experimental models: Organisms/strains		
Mouse, adult > 8 weeks: Sex and strain are not relevant for this protocol	Charles River Laboratories Germany	N/A
Software and algorithms		
Phosphorescence data analysis software	Custom made	Upon request from SAV
Other		
Bonding agent (One Coat 7 UNIVERSAL)	Coltène/Whaledent AG	Cat#60019539
Cannula 26 G	B.Braun Medical AG	Cat#4665457
Dental composite	Ivoclar Vivadent Schweiz AG	Cat#595979WW
Dental curing light	Woodpecker®	LED.F
Dental drill	Rotatec GmbH	Cat#H-4-002 HP
Microbrushes black	Coltène/Whaledent AG	Cat#7634
PortexTM Fine Bore LDPE Tubing	Smiths Medical	Cat#800/100/100
Sapphire glass window (custom-made)	Powatec GmbH	N/A
Shaver	Heiniger AG	707-210 240V EU; 707-211 240V GB
Spectrophotometer NanoDrop®	Thermo Fisher Scientific	ND-1000
Sugi®	Kettenbach GmbH	Cat#31603
Syringe (10 µL, Hamilton)	Hamilton	Cat#80330
Syringe (30 G needle)	B.Braun Medical AG	Cat#9151125S
Tissue adhesive (Histoacryl®)	B.Braun Medical AG	Cat#1050060
Other		
2-photon microscope	Custom made	(Mayrhofer et al., 2015)
Femtosecond laser: Chameleon Discovery	Coherent	N/A
Imaging software: ScanImage 3.8	Vidrio Technologies	N/A
LabView 2012	National Instruments	N/A

MATERIALS AND EQUIPMENT

Microscope

We use a custom-built two-photon microscope (Mayrhofer et al., 2015) with a 20× water-immersion objective (W-Plan-Apochromat 1.0NA DIC, ZEISS, WD = 1.8 mm) and a tunable femtosecond laser (Chameleon Discovery, 80 MHz repetition rate, ~100 fs pulse length, 1.6W maximal power) as an excitation source. The microscope is controlled by a suite of custom-written programs based on ScanImage (Version 3.8) (Pologruto et al., 2003) and LabView (National Instruments).

Alternatives: The protocol described in this contribution is compatible with any two-photon microscopy setup suitable for 2PLM. To the best of our knowledge, presently only two commercial systems, by Bruker and by ISS, are capable of the 2PLM experiment. In addition, Becker & Hickl GmbH offers electronic boards that enable 2PLM measurements on a range of commercial scanning microscopes. The key requirement to the system is the ability to carry out two-photon excitation of the probe and measure the subsequent phosphorescence decay in a time-resolved fashion. If the excitation source is a high-repetition rate laser oscillator, necessary excitation gates (trains of femtosecond pulses) can be generated using electro-optical modulators (see, e.g., (Finikova et al., 2008; Sakadžić et al., 2010; Kazmi et al., 2013)), acousto-optical modulators (e.g., (Parpaleix et al., 2011)) or by rapid scanning the beam over a narrow slit (e.g., (Spencer et al., 2014)). Phosphorescence decay measurements can be performed either in photon counting/binning mode (Finikova et al., 2008) or in analog mode (Parpaleix et al., 2011) using a suitable photomultiplier (PMT) or avalanche photodiode (APD).

Reagent	Final concentration	Amount
Midazolam	1.66 mg/mL	1 mL
Medetomidine	0.166 mg/mL	0.5 mL
Fentanyl	0.016 mg/mL	1 mL
Saline	–	0.5 mL

Note: This mixture can be made in batch (3 mL final solution) and stored at room temperature (20°C–25°C) for 30 days. Inject 3 μL/g body weight intraperitoneally.

STEP-BY-STEP METHOD DETAILS

Injection of Oxyphor 2P

Timing: 10–15 min

This section describes two different methods of injection of the probe: intravenous injection for vascular imaging and cisterna magna injection for intravascular and extravascular imaging.

The choice of the probe delivery route determines the site of the pO_2 measurements. Intravascular injection is suitable for measurements in the vasculature. The easiest delivery route in this case is probably *via* the tail vein (see below). Injection into cisterna magna is technically more demanding, but it leads to the distribution of the probe throughout the interstitial space as well as the vasculature, therefore permitting extravascular and intravascular pO_2 measurements.

Note: If you are performing intravenous (i.v.) injection, proceed to steps 1–9. If you are performing injection into cisterna magna, proceed to steps 10–29.

Pause point: It has been shown previously that Oxyphor 2P delivered *via* cisterna magna injection remains in the brain tissue for several days (Esipova et al., 2019). The optimal measurement time frames are 1–48 h for intravascular and 6–24 h for extravascular measurements post injection.

Injection of Oxyphor 2P via the tail vein

1. Weigh the mouse.

2. Calculate the total blood plasma volume (TBV) of the animal. In mice, the TBV can vary between 63 and 80 mL/kg (Diehl et al., 2001). Using the recommended mean value of 72 mL/kg, the blood plasma volume is found as:

$$TBV[\mu L] = w[g] \cdot 72[\mu L / g],$$

where w is the weight of the animal in grams.

3. Calculate the required volume of the stock solution of Oxyphor 2P (V_{ss}) based on its concentration (c_{ss}) and considering the desired final concentration of the probe in the blood (c_b). We recommend the final concentration of 5 μM, in which case the volume is determined as:

$$V_{ss}[\mu L] = \frac{TBV[\mu L] \cdot c_b}{c_{ss}} = \frac{TBV[\mu L] \cdot 5\ \mu M}{250\ \mu M} = \frac{TBV[\mu L]}{50}$$

4. Using aqueous NaCl (0.9%), dilute the stock solution of volume V_{ss} to the final volume of 50 μL.

   Note: It is easier to inject larger volumes, considering that injection needs to be performed gradually at a constant speed. However, injecting too much solution can harm the animal (Diehl et al., 2001). 50 μL is a convenient compromise.

5. Fill a syringe with the prepared solution of Oxyphor 2P. For i.v. injections use a 30G needle.

   ⚠ CRITICAL: Avoid having air bubbles in the syringe.

6. Anaesthetize the animal with isoflurane (4% induction in an oxygen/air mixture (30%/70%)).
7. Place the mouse on a heating blanket and reduce the isoflurane concentration to 1.5%–2%.
8. Warm up the tail using warm water (about 40°C–45°C) or a heating lamp to dilate the tail vein (duration of warming: ~30–45 s).

   ⚠ CRITICAL: Do not overheat.

9. Once the vein is clearly visible, align the needle parallel to the tail vein with the needle bevel facing up and insert the needle into the vein in the direction of the animal and inject the solution at a rate of ~300 μL/min.

   Note: If the needle missed the vein, the injected solution, which is deep green in color, will localize near the injection site and will not distribute throughout the vascular system. The injection will need to be repeated in a location more proximal to the animal body.

   Note: Upon successful injection, Oxyphor 2P will distribute throughout the vascular system within seconds. Imaging can be performed for several hours after injection.

   Alternatives: Intravascular delivery can be performed *via* other vascular access routes (e.g., retro-orbital injection or injection into the femoral vein (requires catheterization)).

Injection of Oxyphor 2P via cisterna magna

The protocol for intracisternal injections follows Ueda et al. and Furlan et al. (Ueda et al., 1979; Furlan et al., 2003).

Note: The injection is best performed by two people: one person inserts the needle, another performs the injection.

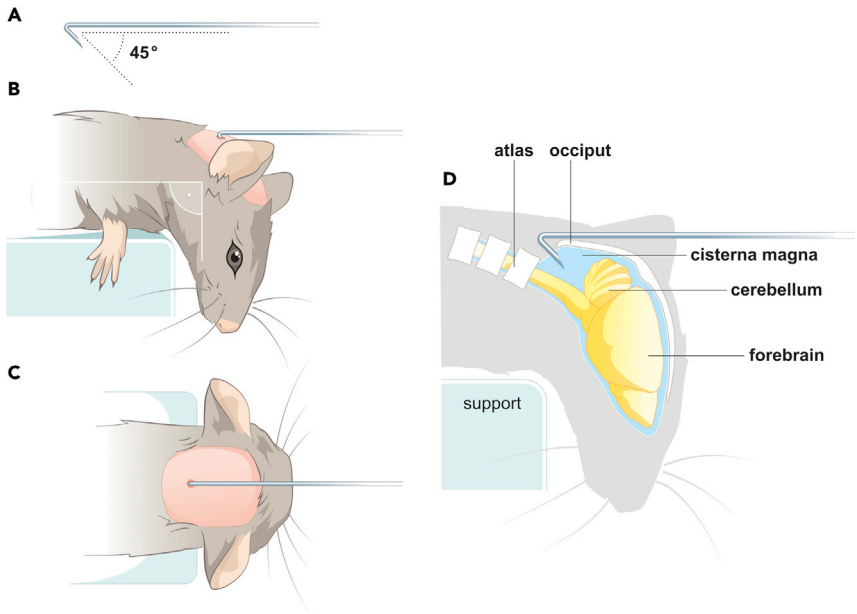

Figure 2. Cisterna magna injection through the intact skin

(A) A needle hook made of a 26G needle.

(B and C) Correct positioning of the mouse and puncture site for cisterna magna injection through the intact skin (pink area): Side view (B), Top view (C). The head is bent downward over the edge of a support box.

(D) Schematic of the sagittal cross-section illustrates the correct placement of the needle for cisterns magna injection.

10. Using tweezers, extract the metal cannula from a 26G syringe needle, removing the plastic adapter for attachment to the syringe.
11. Draw a mark on the needle stem 3–3.5 mm away from the tip.
12. Use a large forceps to bend the needle at the mark, forming a hook. The bevel should face the inside of the hook (Figure 2A).
13. Disinfect the hook by dipping it into aqueous ethanol (70%).
14. Rinse and flush the hook with Ringer solution.
15. Connect the hook to a 45 cm-long polythene tubing (I.D. 0.28 mm, Smiths Medical).
16. Connect the other side of the polythene tubing to a 10 μL syringe (Hamilton).
17. Fill the tubing with Ringer solution by drawing it in using the syringe.
18. Draw in the solution of Oxyphor 2P for cisterna magna injection slightly in excess of the desired amount, e.g., 10.5–11 μL instead 10 μL.

⚠ CRITICAL: Allowing a small bubble of air between the Ringer solution in the tube and the solution of the Oxyphor 2P probe helps to prevent mixing of the solutions and makes it easier to visually detect the amount of injected volume. On the other hand, drawing in a slight excess of the solution of the probe helps to avoid unintentional injection of the air bubble into the animal.

19. Anaesthetize the animal with isoflurane (4% in an oxygen/air (30%/70%) mixture for induction).
20. Place the mouse on a heating blanket and reduce the isoflurane concentration to 1.5%–2%.
21. Shave the neck region of the animal.
22. Place the animal on its abdomen on a support stage (e.g., a box from pipette tips, ~12.4 × 8 × 6 cm, Width: 8.5 cm, Height: 6.2 cm) and bend its head downward over the edge of the box (Figures 2B–2D).
23. By placing the mouse's nose into the isoflurane tube the head is secured in the head-down position and has not to be further fixed.

24. Carefully fix the mouse body with surgical tape on the support stage.
25. Define the injection site (see the note below and Figures 2B–2D).
26. Disinfect the skin at the injection site (Kodan®).
27. Inject 10 μL of the probe solution at a constant rate of approximately 5 μL/min.

Note: The needle needs to be inserted into the gap between the occiput and the atlas vertebra (Figure 2D). Direct the needle tip along the midline drawn from the back of the head toward the neck, holding the stem of the hook parallel to the surface of the occiput, until the hook meets the end of the occiput bone. Insertion of the needle into the gap between the occiput and atlas vertebra should be done without applying excessive force. After the insertion, the stem of the needle hook should be positioned close to the surface of the occiput. Any rotations or other movements of the needle should be avoided. (Figures 2B–2D).

⚠ CRITICAL: Stable positioning of the needle stem (close to the surface) is crucial for successful injection. Holding the needle with a forceps can help the injection. In case of a failed cisterna magna injection, the animal should be carefully monitored and if there are no signs of pain and distress the injection can be repeated in the same animal after 48 h.

28. After completing the injection, keep the needle inserted for a few seconds before removing it.
29. Let the animal wake up and wait for at least 45 min before imaging. The intermission serves as a recovery phase for the animal and allows for distribution of Oxyphor 2P throughout the interstitial space (Iliff et al., 2012).

Note: If you are performing imaging in anesthetized animals, proceed to steps 30–33. If you are performing imaging in awake animals, proceed to steps 34–36.

Preparation for imaging of anaesthetized animals

Timing: 5–10 min

This section describes animal preparation for imaging under isoflurane anaesthesia.

30. Anaesthetize the animal with isoflurane (4% in an oxygen/air (30%/70%) mixture for induction).
31. Place the animal on a heating blanket and reduce the concentration of isoflurane to 1.5%–2%.
32. Use a microbrush, aqueous ethanol (70%) and water to clean the cranial window of any deposits.
33. Position the animal under the microscope and fix it by its head post, leaving it on the heating blanket. Maintain the anesthesia at a reduced level (1.5%–2% isoflurane).

⚠ CRITICAL: During imaging the animal should breathe normal air (21% O_2). Higher concentrations of O_2 in the inhaled mixture could lead to abnormally high tissue pO_2 values.

⚠ CRITICAL: Keep in mind that anesthesia can affect the brain oxygen levels. For example, isoflurane, which is a known vasodilator, can cause an increase in the brain tissue oxygenation (Lyons et al., 2016). For comparing different experiments, it is crucial to conduct them using the same anesthesia.

Preparation for imaging in awake animals

Timing: 5–10 min

This section describes animal preparation for awake imaging.

34. Position the animal under the microscope and carefully affix its head without inducing stress to the animal.
35. Use a microbrush, aqueous ethanol (70%) and water to clean the cranial window of any deposits.
36. Anaesthetize the animal with isoflurane (4% in an oxygen/air (30%/70%) mixture for induction).

Note: Animals that undergo awake imaging don't have to be anesthetized to clean the cranial window.

⚠ CRITICAL: It is important to ensure that the head post of the animal is well fixed head does not move during imaging, since movements in the imaging plane caused by animal locomotion or other type of activities (e.g., licking) can affect the spatial accuracy of the measured pO_2 values. In case fixation is insufficient to completely eliminate motion artifacts, it might be useful to include a motion detector into the setup that would allow rejection of the data obtained during motion. Additional information on 2PLM in awake animals can be found in e.g., Şencan et al., Li et al. (Li et al., 2019; Sencan et al., 2020).

Imaging parameters

This section describes spectral and temporal parameters relevant to and optimal for oxygen imaging.

The imaging procedure starts with the defining a pattern of points in a selected plane. The laser beam will then step through these points to generate the oxygen image. In particular, on each point the laser beam will irradiate the sample for a fixed time (excitation gate) and then will be turned off for a longer time interval to allow for the collection of phosphorescence (phosphorescence collection period). This excitation/collection pattern is repeated for a selected number of cycles to increase the SNR. The details of the imaging procedure are provided below.

The following parameters are appropriate for imaging phosphorescence of Oxyphor 2P:

Excitation gate:	10 μs (800 fs pulses at 80 MHz repetition rate).
Phosphorescence collection period:	260 μs.
Excitation wavelength:	960 nm.
Emission detection range:	740 nm < λ < 900 nm.
Number of cycles (M):	adjust to reach the desired SNR (see below).

Alternatives: Other wavelengths can be used for excitation of Oxyphor 2P. For the spectral properties of Oxyphor 2P see Esipova et al. (Esipova et al., 2019).

Selecting excitation power

This section describes the theoretical background and control experiments for the choice of the excitation power for oxygen imaging.

Too low excitation power will result in poor SNR, while using excessive power can overwhelm the detector, lower spatial resolution and possibly lead to tissue photodamage. It is advised to perform tests to define the power range appropriate for imaging on your particular microscope prior to performing the actual imaging experiments.

Definitions

Signal-to-noise ratio (SNR).

In the shot noise limit (photon counting detection) signal-to-noise ratio is calculated as:

$$SNR = \sqrt{N},$$

where N is the total number of photons (counts) per phosphorescence decay. Note that N should not include the dark noise, i.e., the integral under the baseline B in the fitting equation (see Data Analysis). Photon counting noise is the lowest possible noise achievable in phosphorescence decay measurements. In non-photon counting systems noise levels are always higher, and they depend on the imaging equipment. When multiple decays are averaged, the SNR is still calculated from the total number of photons, i.e., using the sum of the decays.

Detector linear range and saturation

Excitation power should be adjusted such that during imaging the signal intensity does not exceed the limits specified by the detector manufacturer. In the case of photon counting detection using photomultipliers (PMTs), the acceptable count rates are frequently referred to as the PMT *linear range* (usually up to $\sim 10^6$–10^7 counts/s). Within that range arrival of each individual photon is detected, while at higher signal intensities some photons may be missed, which will cause signal distortion and inaccurate determination of the phosphorescence lifetime.

For non-photon counting systems the upper limit corresponds to a certain value of the detector photocurrent, which is specific for each type of hardware. Exceeding that limit similarly will lead to signal distortion and will result in systematic errors in the phosphorescence lifetime determination.

In the limit of very high light (phosphorescence) intensities, the detector's signal becomes insensitive to further increases in the light levels - a phenomenon referred to as *detector saturation* (see Figure 4B for an example of traces exhibiting detector saturation).

Depending on the microscope system, the user may or may not be warned automatically by the imaging program if the detector's linear range has been exceeded. It is advised to implement such control to avoid detector saturation during imaging and errors in pO_2 quantification.

Even when working within the detector's linear range, using excessive excitation power may lead to the saturation of the probe's triplet state within the diffraction-limited volume, leading to a decrease in spatial resolution. This phenomenon has been discussed previously (Sinks et al., 2010). In brief, the highest spatial resolution is achieved when the detected signal originates only from the probe excited within the smallest possible volume near the focal point, known as the *diffraction-limited volume* (Helmchen and Denk 2005). For each imaging setup and object, there is an excitation power range within which only a fraction of the molecules in the diffraction-limited volume is excited, while almost no excitation occurs outside that volume's boundaries. If the power exceeds that range, probe molecules outside the diffraction-limited volume become excited as well, and the imaging resolution degrades.

A method to test whether the signal emanates exclusively from the diffraction-limited volume, or if this volume has been exceeded, consists of recording the dependence of the phosphorescence decay intensity on the excitation power. We recommend performing a power dependence test prior to conducting the actual imaging experiments, especially if these are your first 2PLM measurements with Oxyphor 2P. Once the appropriate power range for a given object type (e.g., mouse brain) has been identified, imaging of similar objects can proceed without repeating the test. However, the power dependence test should be repeated if imaging parameters (e.g., excitation gate duration) or components of the optical system (e.g., laser, objective lens, optical filters etc.) are changed.

To perform the power dependence test, follow the steps below:

37. Select a measurement location (e.g., within a blood vessel at a selected depth), set measurement parameters (see above) and record a phosphorescence decay using an arbitrary number of cycles M (e.g., M=5000) and the maximal acceptable excitation power P_{max} (see Note below).
38. Adjust the detector gain to maximize the signal, while ensuring that the entire trace is contained within the detector's linear range (see definitions above).
39. Adjust M so that the SNR in the data is sufficiently high (e.g., SNR>60 in the case of photon-counting detection).
40. Record phosphorescence traces while decreasing the excitation power P stepwise in the range $0<P<P_{max}$, keeping all the other imaging parameters unchanged. 7–8 excitation power steps should be sufficient (Figure 3A).
41. Select the sections of the signal traces corresponding to the phosphorescence decays (i.e., starting ~5 μs after the end of the excitation pulse). Analyze the resulting phosphorescence decays (see quantification and statistical analysis). Subtract the corresponding baseline terms (B) from each decay and calculate the areas (*A*) under the resulting decays without baselines (Figure 3B). Areas *A* represent the decay's integrated intensities.
42. Plot areas *A* as a function of the excitation power (P) in log/log coordinates (e.g., log(*A*) *vs* log(P), Figures 3C and 3D). Choose the power region where the slope of the plot is ~2.00 (1.95<slope<2.05). This region corresponds to the excitation within the diffraction-limited volume and to the maximal imaging resolution.

Note: Working at higher powers will give more signal and boost the imaging speed, however at expense of imaging resolution. In practice, a compromise between the resolution and speed can be chosen depending on the concrete goal of the experiment.

Note: Control of excitation power is implemented differently in different microscope systems. If the power is adjusted prior to the beam entering the microscope, it is recommended to measure the beam power by an optical power meter inserted in the optical path immediately before the microscope. In this case, the measured power will not match the actual incident power on the sample (after the objective), but will be proportional to its values, which is sufficient for the purpose of the power-dependence experiment. If power control is performed inside the microscope, power measurements might need to be performed after the microscope objective. Either way, power measurements should be performed with the gating device (Pockels cell or acousto-optical modulator) in the fully open position.

Note: Typically, the maximal power P_{max} is chosen based on the environmental considerations, i.e., to avoid overheating of the sample and to minimize phototoxicity. This parameter is specific for each imaging experiment and microscope/laser system. This subject has been addressed in a recent study (Wang and Xu 2020)).

Note: At low excitation powers phosphorescence decays may exhibit low SNR, which will result in the power dependence plot being noisy and thus poorly defined (see Figure 3D as an example). The corresponding portion of the plot should be discarded.

Visualizing the vasculature

Timing: 5 min

This section describes the procedures for visualizing the vasculature as spatial reference for the following oxygen imaging steps.

A large (e.g., 100 × 100 μm) field of view image (or a 3D stack of images at different depths) of the vasculature provides a convenient reference framework for the selection of locations for oxygen measurements. The phosphorescence of Oxyphor 2P can be used as a source of contrast to identify

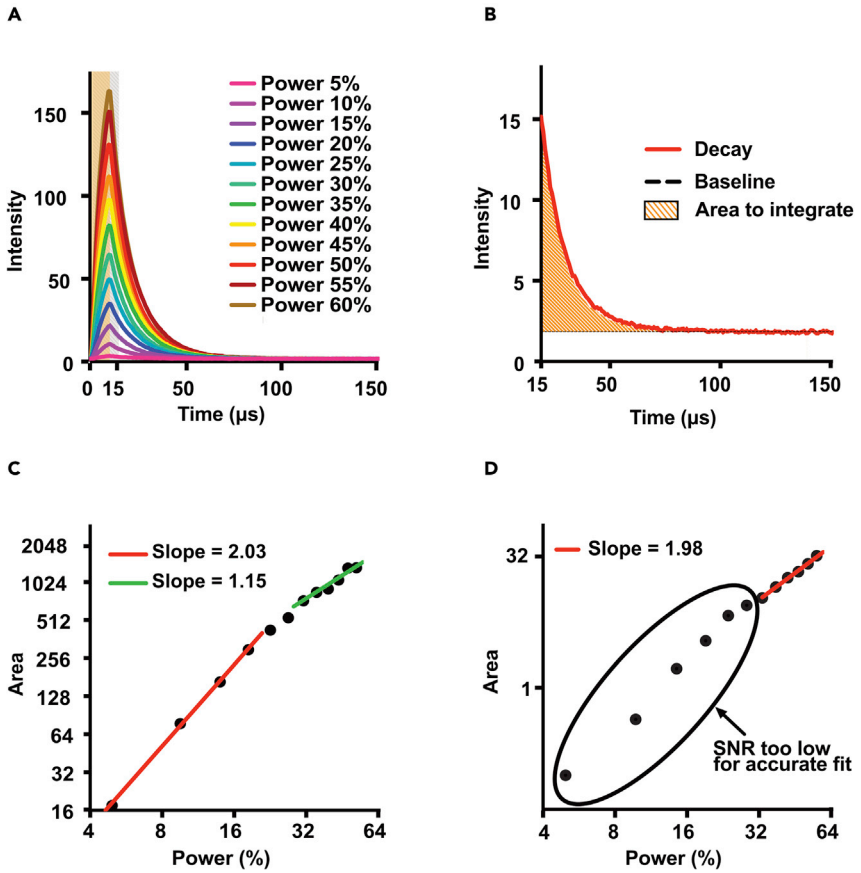

Figure 3. Power dependency tests

(A) Example of phosphorescence traces acquired using progressively higher excitation powers. The yellow region corresponds to the excitation-ON phase in the trace (10 µs). The gray-shaded area marks additional 5 µs after the end of the excitation phase. These 5 µs of the data are removed from the decay to minimize the interference of the detector response function, which in some systems can be slow (microseconds).

(B) Example of decay showing the removal of the first 15 µs, the baseline to be subtracted and the area used to calculate the signal for power dependency plots.

(C) Double logarithmic plot of phosphorescence signal as function of exciting laser power for a sample with good SNR. At lower powers the slope of the fitting line is about 2, as expected for two-photon excitation (red line), while at higher powers the slope is reduced as effect of excitation saturation (green line).

(D) Double logarithmic plot of phosphorescence signal as function of exciting laser power for a sample with poor SNR. At lower powers, the points are too affected by noise to obtain a reliable fit.

the vasculature, particularly upon vascular injection of the probe. Upon cisterna magna injection, additional contrast, e.g., by FITC-dextran (i.v; 50 µL, 70 kDa, 10% in 0.9% NaCl, Sigma) might be needed.

43. Set the excitation and emission wavelengths and image the brain using the regular scanning mode of the microscope, as in conventional fluorescence intensity-based laser scanning microscopy.
44. Define the locations for pO_2 measurements using the vascular image as a reference.

Note: Save the image of the pial vasculature for subsequent imaging sessions. It will serve as a map for future measurements.

Note: Images of the vasculature in the region of interest obtained directly before and after oxygen measurements help to determine whether a movement occurred during the measurements.

Single-point pO_2 measurements

Timing: 5 min

This section describes the procedures for oxygen measurements on pre-selected single points and patterns of points.

45. Select settings for single point pO_2 measurements (see previous section).
46. Select several points within a vessel and/or in the interstitial space and perform a test run in order to estimate the signal strength and SNR.

Note: If the probe was injected intravascularly, the measurements at the locations within the vessels should reveal clear phosphorescence decays (Figure 4), while the measurements outside the vasculature should result in no signal. In the case of cisterna magna injection decays may be present originating from both compartments (Figure 5B, points D and E). Depending on the imaging software, the operator might or might not be able to visualize the phosphorescence traces, such as those shown in Figure 2, at the time of imaging. If this useful feature is not a part of the imaging program, other means of monitoring the signal strength should be present, e.g., an indicator of the signal level with the respect to the detector's linear range and run-time calculation of the SNR.

47. Adjust the laser power so that it falls within the acceptable power range and the signal is within the linear range of the detector (see selecting excitation power).
48. Record the decays.

Note: It is possible to perform measurements in a set of points combined into a pattern, revisiting each point multiple times. Using a pattern is convenient, for example, for assessing pO_2 levels in a large region (e.g., Figure 5C).

Note: Special care is required when selecting excitation power for measurements that encompass both vascular and extravascular compartments, as signal intensities corresponding to these two compartments can be significantly different. In this case, the excitation powers should be chosen such that the signal levels in the two compartments are comparable.

EXPECTED OUTCOMES

This protocol describes pO_2 measurements in the vasculature and interstitial space of the cortical tissue in the mouse brain. Phosphorescence decays are measured in selected points, and the decay times are used for calculation of pO_2. Both intravascular and extravascular measurements can be performed either in individual locations or in grid-like patterns, forming region-wise pO_2 maps.

In the cortex of an awake mouse the mean pO_2 value is ~70 mmHg in the penetrating arterioles (varying in the range of 50–100 mmHg) and ~40 mmHg in the surfacing venules (varying in the range of 20–60 mmHg) (Lyons et al., 2016). In the capillaries the pO_2 values are distributed over a wide range: 5–100 mmHg (Li et al., 2019). In the extravascular space pO_2 values can reach as low as 3–4 mmHg (Lyons et al., 2016). As mentioned above, oxygen levels in the brain tissue are affected by anesthesia.

QUANTIFICATION AND STATISTICAL ANALYSIS

Timing: 0–10 min (depending on the imaging software).

The average time required for single-exponential fitting of a phosphorescence decay, consisting of 300–500 data points, and calculation of pO_2 is <10 ms. Therefore, data analysis is usually performed

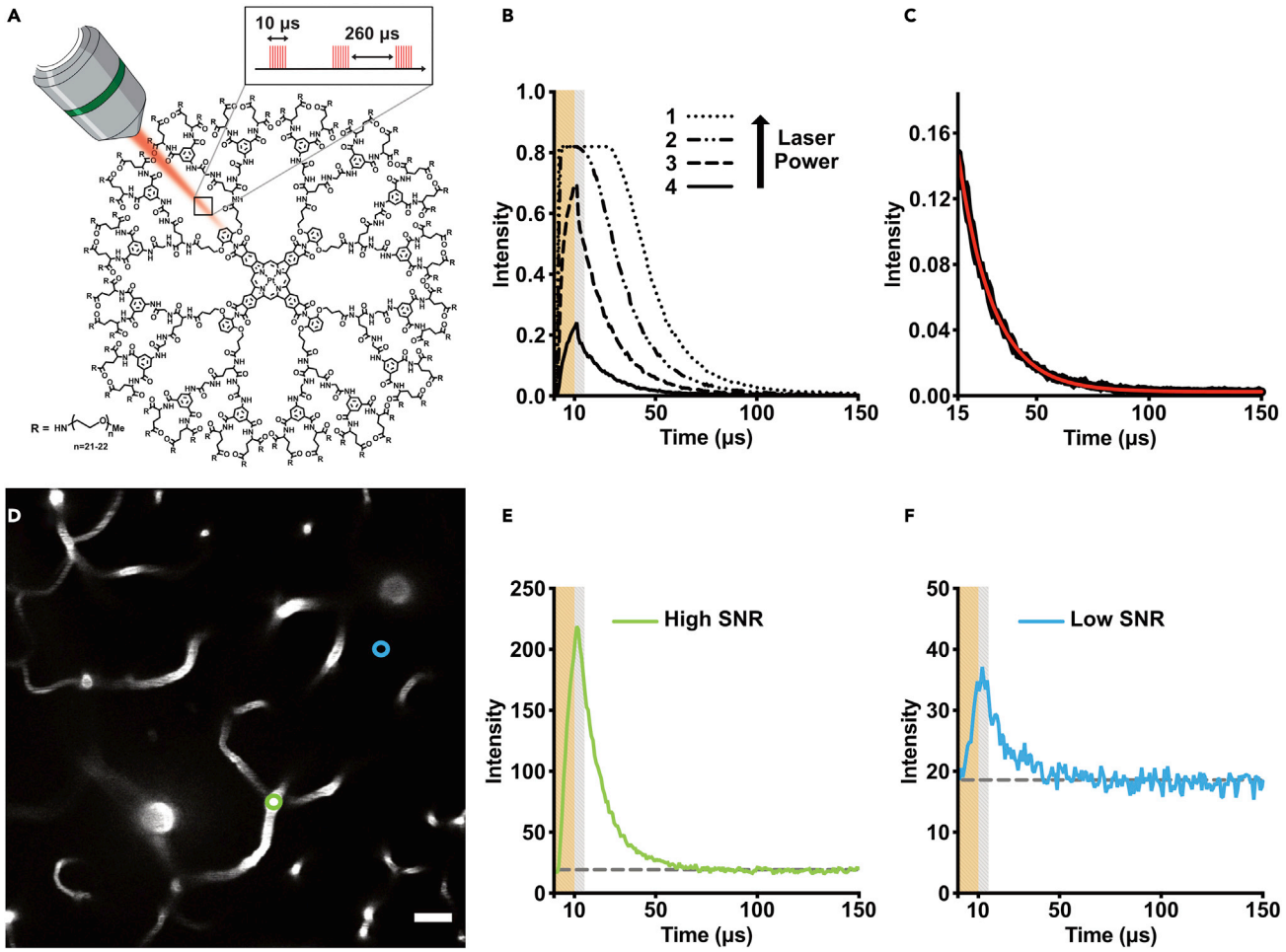

Figure 4. Recording and analyzing phosphorescence decays

The phosphorescence decays are shown as they are presented by the imaging software in the authors' laboratory. Other imaging programs may not be able to allow visualization of the phosphorescence decay data at the time of imaging.

(A) Oxyphor 2P is excited by a 10 µs-long train of femtosecond pulses (150 fs, 80 MHz rep. rate). The excitation is followed by a 260 µs-long data collection period, during which the phosphorescence is detected. The excitation/detection cycles are repeated multiple times in order to increase the SNR.

(B) Example of phosphorescence traces acquired using progressively higher excitation powers. The yellow region corresponds to the excitation-ON phase in the trace (10 µs). The gray-shaded area marks additional 5 µs after the end of the excitation phase. These 5 µs of the data are removed from the decay to minimize the interference of the detector response function, which in some systems can be slow (microseconds). At higher excitation powers the detector response becomes saturated, which is manifested by the truncation of the signal near the peak intensities (traces 1 and 2).

(C) Phosphorescence decay and the fit to a single-exponential function (red line, see quantification and statistical analysis). The resulting phosphorescence lifetime (τ) is used for the calculation of pO_2.

(D) Image of the vasculature used to select the point for pO_2 measurements shown in (E) and (F).

(E and F) Examples of phosphorescence traces corresponding to high and low SNR in the data. Both decays where acquired in the location marked by the blue circle in figure D, using different excitation powers to control the SNR. The gray dashed horizontal lines represent the constant background due to electronic noise and stray light (see quantification and statistical analysis). Scale bar 20 µm.

on-the-fly by the imaging software, and the phosphorescence lifetime/pO_2 images are displayed virtually instantaneously upon data acquisition. In that case, no additional time is required for the analysis. However, some programs collect data and require manual post-processing, in which case additional time is needed for transferring the data to a processing station and executing the analysis script.

Below we summarize the operations that typically comprise the data analysis routine to obtain the pO_2 value from a phosphorescence decay.

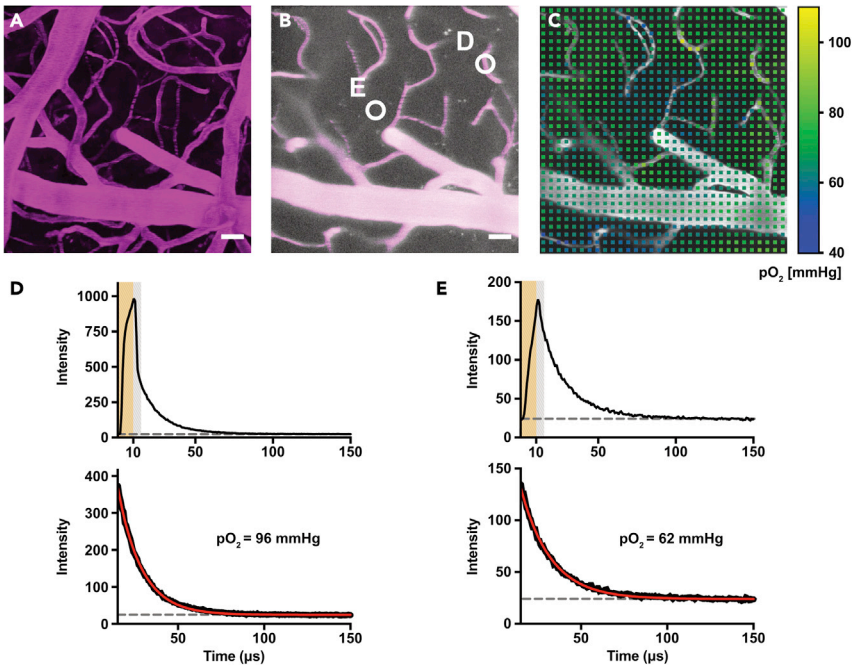

Figure 5. Examples of pO_2 measurements performed after cisterna magna injection of Oxyphor 2P and i.v. injection of FITC-dextran

(A) Maximal intensity projection of a Z-stack of the vascular network imaged using FITC-dextran fluorescence.

(B) Dual-channel image (magenta = FITC-dextran channel, white = Oxyphor 2P channel) of a selected plane along the stack. While FITC-dextran is localized in the vessels only, Oxyphor 2P is present both in the vascular and extravascular space. For better visualization of the extravascular contribution, the image of the phosphorescence channel was converted to logarithmic scale before merging.

(C) Color-coded grid-like image of pO_2 values superimposed on the fluorescence intensity image shown in (B) (FITC-dextran channel).

(D and E) Phosphorescence decays corresponding to the vascular (D) and extravascular (E) points. The signal in D exhibits a rapid drop in intensity following the excitation phase (gray shaded area) due to the fluorescence of FITC-dextran, which could not be removed fully by optical filtering. This fluorescence disappears almost instantaneously (nanoseconds) after the excitation pulse. In (E) fluorescence is not present. After removing the excitation phase (yellow) and the subsequent 5 µs of the data (gray), the remaining traces (D and E, lower graphs) correspond solely to the phosphorescence of Oxyphor 2P in the respective compartments. These phosphorescence decays are used for fitting and phosphorescence lifetime determination. The gray dashed horizontal lines represent the constant background due to electronic noise and stray light (see quantification and statistical analysis). Scale bars 20 µm.

1. Fit the phosphorescence decay starting at 5–10 µs after the end of the excitation pulse using a single-exponential form:

$$I(t) = I_0 \cdot e^{-t/\tau} + B$$

where $I(t)$ is the phosphorescence intensity as a function of time (t), I_0 is the decay initial intensity (or initial amplitude), τ is the phosphorescence decay time and B is a constant baseline term. Fitting is usually performed using the non-linear least squares method implemented as the Marquardt-Levenberg algorithm.

2. Convert the lifetime τ to pO_2 using the expression:

$$pO_2(\tau, T) = \frac{1}{k_q^0 + \beta T} \cdot \left(\frac{1}{a \cdot \tau^p} - \frac{1}{\tau_0^0 + \alpha T} \right)$$

where τ is obtained by fitting, T is temperature in °C, and k_q^0, α, β, $\tau^0{}_0$ and p are empirical constants determined by independent calibrations and supplied with the probe:

- τ_0^0 = 3.96441 × 10^{-5} s.
- k_q^0= 106.1337.
- a = 14.8.
- p = 1.265776950.
- β = 18.89122.
- α = 5.94517 × 10^{-8}.

Note: The equation shown above is further refined compared to the expression that was reported originally in (Esipova et al., 2019).

LIMITATIONS

Probe retention

Injection of Oxyphor 2P *via* cisterna magna allows pO_2 imaging in the brain during several days, whereas pO_2 imaging after i.v. injection is limited to several hours.

Upon injection of Oxyphor 2P into the cisterna magna, signals originating from both the extracellular space and vasculature can be observed, and the distribution of the probe between the compartments changes over time. The origins and the dynamics of these distributions are not fully understood and are currently being investigated. Importantly, cisterna magna injection enables extravascular imaging, but it does not lead to exclusively extravascular localization of the probe.

Imaging depth

Depth resolution in two-photon imaging has been extensively discussed in the literature (Helmchen and Denk 2005). Due to tissue scattering and endogenous absorption, two-photon excitation at higher depths requires progressively higher laser fluxes (powers), which enhances out-of-focus excitation and degrades imaging resolution. For Oxyphor 2P in our experimental setup the maximal imaging depth has been estimated to be ~600 μm (Esipova et al., 2019), however this number is a function on the excitation wavelength and of various parameters of imaging optics as well as of specific properties of the imaged object.

Secondary excitation

When working with samples that contain significant amounts of fluorophores that can be two-photon excited simultaneously with Oxyphor 2P and whose fluorescence emission spectra overlap with one-photon absorption spectra of Oxyphor 2P, Oxyphor 2P molecules can be indirectly excited by the fluorescence photons - a phenomenon known as secondary excitation *via* emission-reabsorption. Secondary excitation can excite Oxyphor 2P molecules outside the diffraction-limited volume (see below) and hence lead to a decrease in spatial resolution. To minimize secondary excitation, it is recommended to keep the concentration of potentially interfering fluorophores as low as possible.

Manual expertise

Intravenous injections are relatively simple to perform. However, cisterna magna injections through the intact skin require more training. Incorrectly performed cisterna magna injections usually lead to the lack of signal during imaging.

TROUBLESHOOTING

Problem 1

During imaging (see single-point pO2 measurements, steps 45–48), the SNR is insufficient to achieve the desired accuracy in pO_2 determination.

Potential solution

Considering the imaging parameters described above (see step-by-step method details) and the ideal case of shot noise-limited detection (see selecting excitation power), the minimal number of photons required to achieve the accuracy of ± 1 mmHg near pO_2=20 mmHg is ~4200, which corresponds to a SNR of ~65 (Esipova et al., 2019). To determine the actual relationship between the accuracy in the determination of pO_2 and imaging parameters in your system, it is recommended to perform test experiments using model systems, e.g., a fully deoxygenated solution of Oxyphor 2P (pO_2=0) and/or a solutions equilibrated with air (pO_2~150 mmHg at 23°C).

To increase the SNR:

- Increase the laser power (see selecting excitation power).
- Increase the number of acquisition cycles (M).
- Increase the concentration of Oxyphor 2P.

> *Note:* Dedicated toxicological studies of Oxyphor 2P have not been carried out. However, concentrations of up to 20 μM (final concentration in the blood) have been tested and showed no signs of toxicity. We recommend not to exceed 10 μM concentration.

Problem 2

During imaging (see single-point pO2 measurements, steps 45–48), the spatial resolution is suboptimal and/or the signal is observed from the extravascular space near a vessel while probe was delivered i.v.

Potential solution

Decrease the excitation power to ensure that the problem is not caused by saturation of the excitation volume (see selecting excitation power).

Problem 3

After injection in the cisterna magna, the contrast between vasculature and tissue is not sufficient to visualize the vascular network (see visualizing the vasculature, steps 43–44).

Potential solution

Increase the contrast by performing an i.v. injection of FITC-dextran (50 μL, 70 kDa, 10% in 0.9% NaCl, Sigma).

Problem 4

During imaging (see single-point pO2 measurements, steps 45–48), the SNR is unusually low compared to the previous experiments performed in the same animal.

Potential solution

Glass window might be covered with debris. Clean the window using ethanol and a microbrush.

Problem 5

During imaging following cisterna magna injection (see visualizing the vasculature, steps 43 and 44), the extracellular signal appears uniform and can be easily confounded with background noise.

Potential solution

Solutions to this problem are based on:

- Increasing the phosphorescence signal:
- Wait for the probe to properly diffuse in the extracellular space (about 3–6 h post injection).
- If point 1 is not sufficient, repeat the experiment injecting a higher amount of probe.

- Subtracting the noise:
- Collect the phosphorescence image.
- Turn off the laser and collect a "dark image" using identical imaging parameters.
- Subtract the background image from the phosphorescence image to remove the dark noise contribution.

RESOURCE AVAILABILITY

Lead contact

Further information and requests for resources and reagents should be directed to and will be fulfilled by the lead contact, Bruno Weber (bweber@pharma.uzh.ch) and Sergei Vinogradov (vinograd.upenn@gmail.com).

Materials availability

Probe Oxyphor 2P is available from the Resource for *Oxygen Imaging by Phosphorescence Quenching* (Grant U24 EB028941 from the NIH USA; Technical Contact: Sergei A. Vinogradov [vinograd.upenn@gmail.com]).

Data and code availability

Custom code for 2PLM of oxygen is available from the Resource for Oxygen Imaging by Phosphorescence Quenching (Grant U24 EB028941 from the NIH USA; Technical Contact: Sergei A. Vinogradov [vinograd.upenn@gmail.com]).

ACKNOWLEDGMENTS

We gratefully acknowledge grant U24 EB028941 from the NIH USA (S.A.V.) and grant 310030_182703 from the Swiss National Science Foundation (B.W.).

AUTHOR CONTRIBUTIONS

Conceptualization, S.A.V. and B.W.; Methodology, E.E., L.R., M.T.W., J.C., T.T., S.A.V., and B.W.; Software, S.A.V. and L.R.; Formal Analysis, E.E., L.R., and S.A.V.; Investigations, E.E., M.T.W., J.C., and L.R.; Writing - Original Draft, E.E. and L.R.; Visualization, E.E., L.R., and B.W.; Writing - Review & Editing, all authors; Funding Acquisition, S.A.V. and B.W.

DECLARATION OF INTERESTS

We have no conflict of interest to declare.

REFERENCES

Briñas, R.P., Troxler, T., Hochstrasser, R.M., and Vinogradov, S.A. (2005). Phosphorescent oxygen sensor with dendritic protection and two-photon absorbing antenna. J. Am. Chem. Soc. *127*, 11851–11862. https://doi.org/10.1021/ja052947c.

Diehl, K.H., Hull, R., Morton, D., Pfister, R., Rabemampianina, Y., Smith, D., Vidal, J.M., and van de Vorstenbosch, C.; Methods EF of PIA and EC for the V of A (2001). A good practice guide to the administration of substances and removal of blood, including routes and volumes. J. Appl. Toxicol. *21*, 15–23.

Esipova, T.V., Barrett, M.J.P., Erlebach, E., Masunov, A.E., Weber, B., and Vinogradov, S.A. (2019). Oxyphor 2P: a high-performance probe for deep-tissue longitudinal oxygen imaging. Cell Metab. *29*, 736–744.e7. https://doi.org/10.1016/j.cmet.2018.12.022.

Finikova, O.S., Lebedev, A.Y., Aprelev, A., Troxler, T., Gao, F., Garnacho, C., Muro, S., Hochstrasser, R.M., and Vinogradov, S.A. (2008). Oxygen microscopy by two-photon-excited phosphorescence. ChemPhysChem *9*, 1673–1679. https://doi.org/10.1002/cphc.200800296.

Furlan, R., Pluchino, S., Marconi, P.C., and Martino, G. (2003). Cytokine gene delivery into the central nervous system using intrathecally injected nonreplicative viral vectors. Methods Mol. Biol. *215*, 279–290. https://doi.org/10.1385/1-59259-345-3:279.

Helmchen, F., and Denk, W. (2005). Deep tissue two-photon microscopy. Nat. Methods *2*, 932–940. https://doi.org/10.1038/nmeth818. http://www.nature.com/doifinder/10.1038/nmeth818.

Holtmaat, A., Bonhoeffer, T., Chow, D.K., Chuckowree, J., De Paola, V., Hofer, S.B., Hübener, M., Keck, T., Knott, G., Lee, W.C.A., et al. (2009). Long-term, high-resolution imaging in the mouse neocortex through a chronic cranial window. Nat. Protoc. *4*, 1128–1144. https://doi.org/10.1038/nprot.2009.89.

Iliff, J.J., Wang, M., Liao, Y., Plogg, B.A., Peng, W., Gundersen, G.A., Benveniste, H., Vates, G.E., Deane, R., Goldman, S.A., et al. (2012). A paravascular pathway facilitates CSF flow through the brain parenchyma and the clearance of interstitial solutes, including amyloid β. Sci. Transl. Med. *4*, 147ra111. https://doi.org/10.1126/scitranslmed.3003748.

Kazmi, S.M.S., Salvaggio, A.J., Estrada, A.D., Hemati, M.A., Shaydyuk, N.K., Roussakis, E., Jones, T.A., Vinogradov, S.A., and Dunn, A.K. (2013). Three-dimensional mapping of oxygen tension in cortical arterioles before and after occlusion. Biomed. Opt. Express *4* (7), 1061–1073. https://doi.org/10.1364/boe.4.001061.

Kılıç, K., Desjardins, M., Tang, J., Thunemann, M., Sunil, S., Erdener, Ş.E., Postnov, D.D., Boas, D.A., and Devor, A. (2021). Chronic cranial windows for long term multimodal neurovascular imaging in mice. Front. Physiol. *11*, 1–10. https://doi.org/10.3389/fphys.2020.612678.

Li, B., Esipova, T.V., Sencan, I., Kilic, K., Fu, B., Desjardins, M., Moeini, M., Kura, S., Yaseen, M.A., Lesage, F., et al. (2019). More homogeneous capillary flow and oxygenation in deeper cortical layers correlate with increased oxygen extraction. Elife *8*, e42299. https://doi.org/10.7554/elife.42299.

Lyons, D.G., Parpaleix, A., Roche, M., and Charpak, S. (2016). Mapping oxygen concentration in the awake mouse brain. Elife *5*, 1–16. https://doi.org/10.7554/eLife.12024.

Mayrhofer, J.M., Haiss, F., Haenni, D., Weber, S., Zuend, M., Barrett, M.J.P., Ferrari, K.D., Maechler, P., Saab, A.S., Stobart, J.L., et al. (2015). Design and performance of an ultra-flexible two-photon microscope for in vivo research. Biomed. Opt. Express *6* (11), 4228–4237. https://doi.org/10.1364/boe.6.004228.

Lecoq, J., Parpaleix, A., Roussakis, E., Ducros, M., Houssen, Y.G., Vinogradov, S.A., and Charpak, S. (2011). Simultaneous two-photon imaging of oxygen and blood flow in deep cerebral vessels. Nat. Med. *17*, 893–898. https://doi.org/10.1038/nm.2394.

Pologruto, T.A., Sabatini, B.L., and Svoboda, K. (2003). ScanImage: flexible software for operating laser scanning microscopes. Biomed. Eng. Online *2*, 13. https://doi.org/10.1186/1475-925x-2-13.

Roussakis, E., Spencer, J.A., Lin, C.P., and Vinogradov, S.A. (2014). Two-photon antenna-core oxygen probe with enhanced performance. Anal. Chem. *86*, 5937–5945. https://doi.org/10.1021/ac501028m.

Sakadžić, S., Roussakis, E., Yaseen, M.A., Mandeville, E.T., Srinivasan, V.J., Arai, K., Ruvinskaya, S., Devor, A., Lo, E.H., Vinogradov, S.A., and Boas, D.A. (2010). Two-photon high-resolution measurement of partial pressure of oxygen in cerebral vasculature and tissue. Nat. Methods *7*, 755–759. https://doi.org/10.1038/nmeth.1490.

Sencan, I., Esipova, T., Kilic, K., Li, B., Desjardins, M., Yaseen, M.A., Wang, H., Porter, J.E., Kura, S., Fu, B., et al. (2020). Optical measurement of microvascular oxygenation and blood flow responses in awake mouse cortex during functional activation. J. Cereb. Blood Flow Metab. 510–525. https://doi.org/10.1177/0271678x20928011.

Sinks, L.E., Robbins, G.P., Roussakis, E., Troxler, T., Hammer, D.A., and Vinogradov, S.A. (2010). Two-photon microscopy of oxygen: polymersomes as probe carrier vehicles. J. Phys. Chem. B *114*, 14373–14382. https://doi.org/10.1021/jp100353v.

Spencer, J.A., Ferraro, F., Roussakis, E., Klein, A., Wu, J., Runnels, J.M., Yusuf, R., Cote, D., Vinogradov, S.A., Scadden, D.T., et al. (2014). Direct measurement of local oxygen concentration in the bone marrow of live animals. Nature *508*, 269–273. https://doi.org/10.1038/nature13034.

Ueda, H., Amano, H., Shiomi, H., and Takagi, H. (1979). Comparison of the analgesic effects of various opioid peptides by a newly devised intracisternal injection technique in conscious mice. Eur. J. Pharmacol. *56*, 265–268. https://doi.org/10.1016/0014-2999(79)90181-x.

Vanderkooi, J.M., Maniara, G., Green, T.J., and Wilson, D.F. (1987). An optical method for measurement of dioxygen concentration based upon quenching of phosphorescence. J. Biol. Chem. *262*, 5476–5482. https://doi.org/10.1016/s0021-9258(18)45596-2.

Wang, T., and Xu, C. (2020). Three-photon neuronal imaging in deep mouse brain. Optica *7*, 947. https://doi.org/10.1364/optica.395825.

Zuend, M., Saab, A.S., Wyss, M.T., Ferrari, K.D., Hösli, L., Looser, Z.J., Stobart, J.L., Duran, J., Guinovart, J.J., Barros, L.F., and Weber, B. (2020). Arousal-induced cortical activity triggers lactate release from astrocytes. Nat. Metab. *2*, 179–191. https://doi.org/10.1038/s42255-020-0170-4.